In Situ Fourier Transform Infrared Spectroscopic Study of the Conformational Changes of High-Density Poly(ethylene) during the Melting and Crystallization Processes

Yan Xiao,[1] Liangyu Yan,[1] Puming Zhang,[2] Na Zhu,[3] Liang Chen,[1] Peng He,[1] Yanping Wang,[1,4] Xinyuan Shen,[4] Xinyuan Zhu,[1,3] Deyue Yan[1]

[1]*The State Key Laboratory of Metal Matrix Composites, College of Chemistry and Chemical Technology, Shanghai Jiao Tong University, Shanghai 200240, People's Republic of China*
[2]*Department of Biomedical Engineering, Shanghai Jiao Tong University, Shanghai 200030, People's Republic of China*
[3]*Instrumental Analysis Center, Shanghai Jiao Tong University, Shanghai 200030, People's Republic of China*
[4]*State Key Laboratory for Modification of Chemical Fiber and Materials, Donghua University, Shanghai 200051, People's Republic of China*

Received 1 May 2005; accepted 8 July 2005
DOI 10.1002/app.22574
Published online in Wiley InterScience (www.interscience.wiley.com).

ABSTRACT: The conformational analysis of high-density poly(ethylene) (HDPE) during the melting and crystallization processes has been performed by the aid of the time-reserved Fourier transform infrared spectroscopy and multivariate analysis technique. Upon heating, the conformational transition of HDPE takes place, gradually, due to the restraint of crystal lattice, and various conformational transformations can be discerned clearly. However, during the cooling process, HDPE crystallizes very quickly and only one major conformational transition occurs in the crystallization process. The comparison of conformational changes during the melting and crystallization processes exhibits that although the polymer crystallization is the reverse process of polymer melting, there still exist some obvious differences in the conformational transformation between them. © 2006 Wiley Periodicals, Inc. J Appl Polym Sci 100: 4835–4841, 2006

Key words: poly(ethylene); conformational analysis; crystallization; FTIR

INTRODUCTION

Since Keller and coworkers first found the single lamellar structure of poly(ethylene) (PE) by electron microscope, in 1957,[1–3] polymer crystallization theory has been fully developed in the following few decades. To explain the mechanism and essence of polymer crystallization, several different kinds of crystallization models have been put forward in theory.[4–8] On the other hand, many researchers have used various experimental methods to reveal the microscopic structure of semicrystalline polymers and their crystallization processes.[9–12] Currently, a lot of spectroscopic techniques are available to access these aims, and Fourier transform infrared spectroscopy (FTIR) is one of the most widely used methods, because of its versatility in determining composition, configuration, conformation, crystallinity, molecular movement, and so forth.[12–14]

PE is a polymer with the simplest structure and a relatively uncomplicated infrared spectrum; therefore, it has been extensively used to explore the mechanism and essence of polymer crystallization.[15–17] The early work was focused on *n*-alkanes and oligomers. Snyder and coworkers[14,18–20] have reported that three types of nonplanar defects exist in the highest-temperature phase of all the *n*-alkanes by FTIR: "end-gauche," (-t_mg) "kink," (-gtg′- or -gtg-) and "double-gauche" (-gg-). The end-gauche can be observed even in the lower-temperature phases, while the kink conformers are found in the highest-temperature phase. Moreover, the double-gauche defects appear only within a few degrees of the melting points. At the same time, the relation between conformational defects and infrared bands for *n*-alkane has been extensively studied.[18–22] It has been pointed out that the bands at 1340, 1308, and 1352 cm^{-1} correspond to the conformers of -t_mg, -gtg- (-gtg′-), and -gg-, respectively. There are some identical infrared bands for PE and *n*-alkane, because they are structurally alike, except that the methylene segments of the former are much longer than those of the latter, so that it is feasible to use the

Correspondence to: X. Zhu (xyzhu@sjtu.edu.cn).
Contract grant sponsor: National Natural Science Foundation, China; contract grant number: 20574044 20104004.
Contract grant sponsor: State Key Laboratory for Modification of Chemical Fiber and Materials.

aforementioned defect bands, to investigate the conformational changes of PE during the melting and crystallization processes.

It has been well realized that the crystallization of PE consists of the conformation change of macromolecular chains, which seems quite important for the clarification of the essential features of the polymer crystallization. Recently, based on an organized combination of various kinds of time-resolved techniques, such as FTIR, FT-Raman, WAXS, SAXS, WANS, and SANS, Tashiro and coworkers[12,22,23] studied the conformational change of PE in the induction period of crystallization. It has been found that the crystallization of PE-melt into the stable orthorhombic phase occurs via the formation of disordered short trans sequences, and then the transformation and extension of longer and regular trans sequences. However, the problem as how to transform each other for the vaious molecular conformation/defects during the crystallization and melting processes has not yet been solved. Here, we used a new strategy to study the crystallization behavior of PE[24,25]: First, the conformational change of PE during the melting process was recorded continually by time-resolved FTIR spectroscopy. Then, we adopted the same experimental method to follow the tracks of molecular structure change during the crystallization process. By the comparison of these two processes, some interesting results can be concluded.

EXPERIMENTAL

Sample preparation

High-density poly(ethylene) (HDPE) was kindly supplied by Shanghai Jinshan Petrochemical Corp., Shanghai, China. It has a melt flow index of 1.0 g/10 min. A film sample was prepared for FTIR measurement, as thin as possible, to avoid asymmetry of the heating. The operational procedure is casting 3% hot solution of HDPE in xylene on a piece of clean glass, and then vaporizing the solvent at its boiling point. The film of 20 μm in thickness was obtained. To erase the previous thermomechanical history, the film was melted at 160°C for 5 min, and then cooled slowly to room temperature (25°C).

Measurements

The time-resolved FTIR measurements were performed on a Bruker Equinox-55 FTIR spectrometer, equipped with a variable-temperature cell. A film was sandwiched between two KBr plates and heated from 60°C, at a rate of 5°C/min. At the same time, two scans were collected for each spectrum, for every 4 s from 4000 to 400 cm^{-1}, at a resolution of 4 cm^{-1}. The details have been reported previously.[24–29] The curve-fitting procedure was adopted to evaluate the integrated intensity of all bands. Here, the integrated intensity refers to the peak area with baseline.

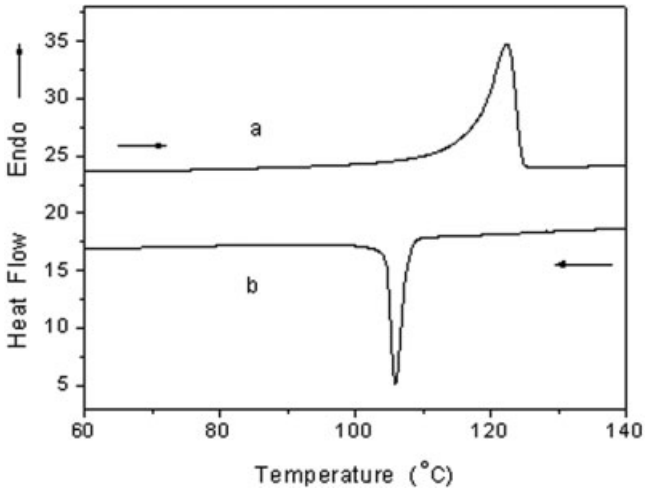

Figure 1 DSC thermograms of HDPE sample during: (a) melting and (b) crystallization processes at 5°C/min.

The IR data were also treated by using principal components analysis (PCA), one of the most commonly used multivariate analysis techniques. PCA model was built by using the Matlab 6.5 software.

The calorimetric measurements were carried out on a Perkin–Elmer Pyris-1 Series differential scanning calorimeter (DSC), under a flowing nitrogen atmosphere. The DSC was carefully calibrated, using In and Pb as standards. A sample of ~5 mg was used, and the heating or cooling rate was 5°C/min. DSC showed that the melting point and crystallization temperature of HDPE were about 122 and 106°C (see Fig. 1).

RESULTS AND DISCUSSION

In the infrared spectra of semicrystalline polymers, some absorption bands disappear in the molten state or in solution. These bands are usually called infrared crystalline bands, which are caused by intermolecular forces in crystal lattice.[30–32] Figure 2(a) gives the infrared spectra of HDPE, at various temperatures in the frequency regions 1480–1440 and 740–700 cm^{-1}. It can be found that the bands at 1472 and 730 cm^{-1} disappear, as the temperature increases to melting point, which is in accordance with the reports in literature.[12,22] Thus, these two bands belong to the infrared crystalline bands, related to the orthorhombic modification of HDPE.[12,22,33–35]

It is worth noting that another three conformational bands of HDPE at 1340 cm^{-1} (-t_mg), 1308 cm^{-1} (-gtg- and -gtg'-), and 1352 cm^{-1} (-gg-) change during the melting process, as in Figure 2(b). Different from those of *n*-alkane,[18–20] all the conformational bands of PE,

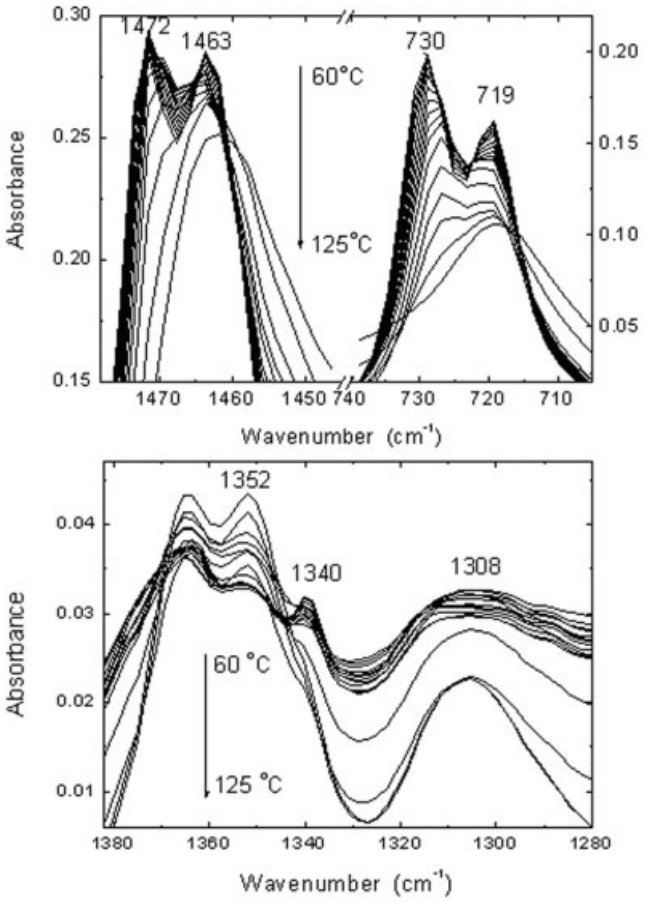

Figure 2 Infrared spectra of HDPE taken as a function of temperature for the melting process: (a) two infrared crystalline bands at 1472 and 730 cm^{-1}; (b) three conformational bands at 1340 cm^{-1} ($-t_mg$), 1308 cm^{-1} (-gtg- and -gtg'-), and 1352 cm^{-1} (-gg-).

mentioned earlier, can be observed even at room temperature. Apparently, much longer methylene chains and the lamellar structure in PE result in a more disorder degree than *n*-alkenes.

Figure 3 presents the plot of the relative intensity of various bands versus temperature (from 60 to 125°C), in which the evolution of relative intensity can be seen more clearly. As described earlier, both 1472 and 730 cm^{-1} bands originate from the intermolecular forces of the orthorhombic form of HDPE; therefore, they are related to the planar zigzag or all-trans conformation ($-t_n-$) of PE chains.[12,22] With the increase of temperature, the absorption of crystalline bands decreases, reflecting the enlargement of gauche conformers. When the temperature is lower than 84°C, the intensity of 1308 and 1352 cm^{-1} bands changes only slightly, whereas the end-gauche conformation ($-t_mg$) at 1340 cm^{-1} increases quickly. Obviously, the end-groups of polymer chains are of high mobility, which is easy to produce the conformational transition. On the other hand, due to the restraint of crystal lattice, the conformational transition of main chains is difficult to occur. Therefore, the major characteristics of HDPE below 84°C are the conformational transformation from all-trans to end-gauche.

As the temperature is higher than 84°C, premelting occurs and the mobility of molecular chains is strengthened greatly, and so the absorption of crystalline bands at 1472 and 730 cm^{-1}, correlating to the high conformational order, diminishes. Because of the growth of gauche conformers, both the all-trans and end-gauche conformations change into other nonplanar defects with high disorder, such as kink and double gauche. In the meantime, some kink gauches also transform into double gauches. Therefore, in the temperature range of 84–110°C, the absorption of 1340 cm^{-1} decreases and the band intensity at 1352 cm^{-1} increases, while the concentration of kink conformer keeps almost unchanged.

Once the temperature arrives at 110°C, some thin lamellae start melting. With the destruction of planar zigzag conformation, the increase of band intensity at 1308 and 1352 cm^{-1} is hastened until the melting point. Finally, when the temperature is higher than 122°C (DSC measurement in Fig. 1 shows it is the melting point of HDPE sample), the sample of HDPE is in a melting phase. Infrared crystalline bands disappear, in which there is no restraint of crystal lattice. All of the molecular chains are in a random coil state, and so the absorption of conformational bands, kink (-gtg- or -gtg'-), and double-gauche (-gg-) diminishes slightly, because of the conformational disordering of HDPE chains, with more continuous g conformers. On the contrary, as a result of the conformational transition from all-trans to end-gauche, the 1340 cm^{-1} intensity increases slightly after the collapse of crystal lattice.

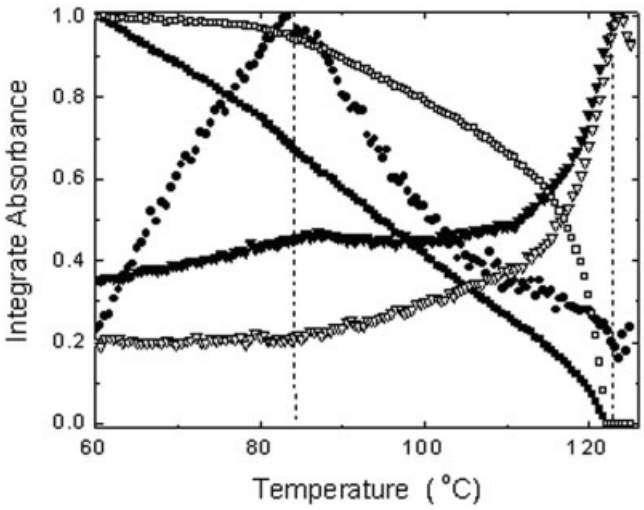

Figure 3 Temperature dependence of integrated absorbance of the bands in the melting process associated with crystalline phase (■ 730 cm^{-1} and □ 1472 cm^{-1}) and conformational defects [● 1340 cm^{-1}: $-t_mg$; ▼ 1308 cm^{-1}: -gtg- (kink); and ▽ 1352 cm^{-1}: -gg- (double-gauche)].

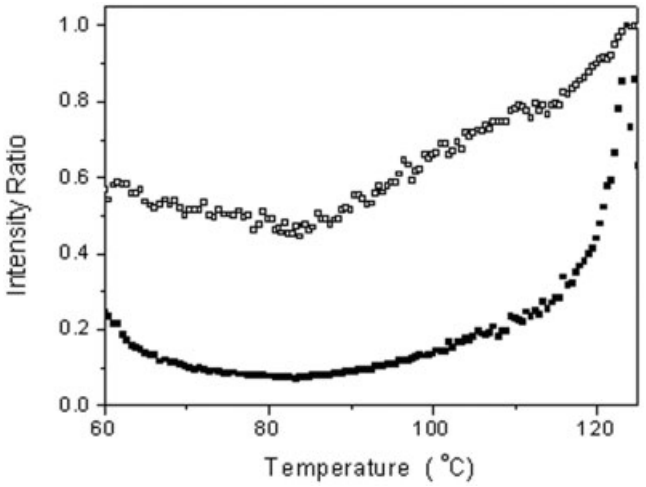

Figure 4 The intensity ratios of different conformational bands versus temperature in the melting process: (a) ■ A_{1308}/A_{1340}: the ratio of kink to end-gauche; (b) □ A_{1352}/A_{1308}: the ratio of double gauche to kink.

To reveal the relationship of those conformational bands, the intensity ratios of different conformational bands after normalization are plotted against temperature. Since the 1308 and 1352 cm^{-1} bands represent the kink and double-gauche conformers respectively, the value of A_{1308}/A_{1340} (A refers to integrated absorbance) can be considered as the concentration ratio of kink to end-gauche. In the same way, the value of A_{1352}/A_{1308} reflects the concentration ratio of double gauche to kink. It can be seen in Figure 4(a) that when the temperature is lower than 84°C, the growth of end-gauche conformers is much faster than that of the kink conformations, and so the intensity ratio of A_{1308}/A_{1340} decreases. However, at high temperature (>84°C), the reverse happens, and so the A_{1308}/A_{1340} value becomes larger. Similarly, Figure 4(b) shows that the intensity ratio of A_{1352}/A_{1308} reduces only slightly at low temperature, while the double gauche increases much faster than the kink conformations above 84°C.

Multivariate analysis is a set of mathematical tools to deal with the large quantities of information extracted from tens or hundreds of measurements, for each sample[36,37]; therefore, it should be very appropriate for using such an approach to analyze IR spectra of melting and crystallization processes. Here, we used the PCA, one of the most commonly used multivariate analysis techniques, to analyze the IR data.[37–40] This approach enables the analysis of the variance in data to be simplified, by extracting the principal components. Figure 5 gives the HDPE heating scores plot of PC1, which accounts for 74.41% of the variance of the spectral data, in the temperature range of 60–125°C, against PC2, which accounts for 14.83%. It can be found that with increase of temper-

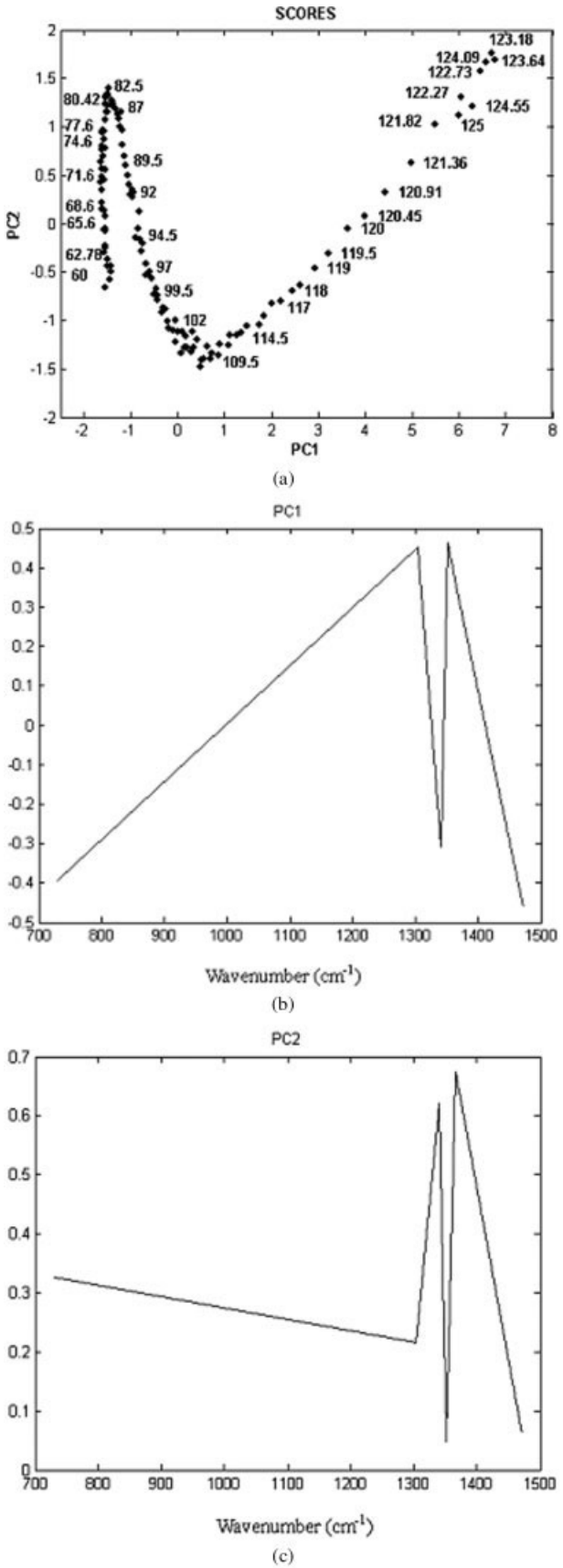

Figure 5 PCA applied to the IR data (a), and plots of PC1 (b), and PC2 (c), during the heating process.

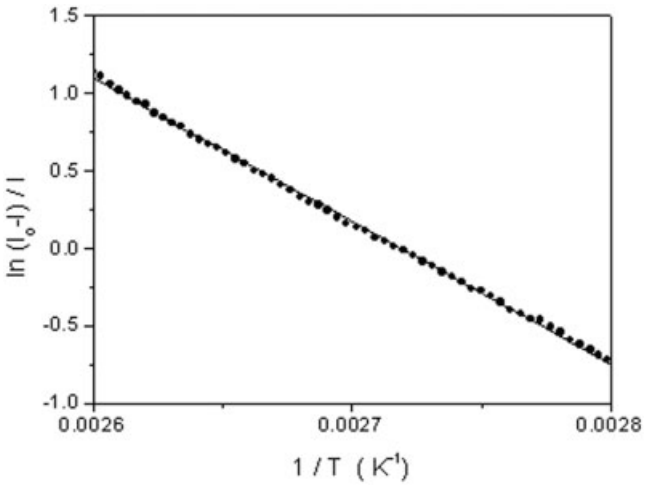

Figure 6 The plot of the intensity of 730 cm^{-1} crystalline band against $1/T$, where T is the temperature.

ature three obvious transitions occur in the vicinity of 83, 110 and 123°C respectively, corresponding quite well to the aforementioned conformational transformations. The multivariate analysis of IR data confirms the multiple conformational transitions, upon heating.

Using the Snyder method, the melting activation energy of HDPE can be calculated.[20,41] Figure 6 gives the plot of the 730 cm^{-1} crystalline band intensity against $1/T$. According to the slope of the straight line, the melting activation energy of HDPE is found to be 79.6 kJ/mol, which is close to the values reported in literature.[42–44]

Polymer crystallization is the reverse process of polymer melting; thus, the information obtained in the melting process must be beneficial to understand the mechanism of polymer crystallization. On the basis of the aforementioned observation of melting process, we further studied the crystallization behavior of HDPE. Figure 7 gives the infrared spectra of HDPE, at various temperatures in the frequency regions of 1480–1450, 740–710, and 1380–1280 cm^{-1}. It can be found that the band at 1463 cm^{-1} begins to split into two bands at 1472 and 1460 cm^{-1} respectively, at about 107°C, during the cooling process. In the meantime, the band at 719 cm^{-1} splits into two bands at 730 and 719 cm^{-1}. This fact demonstrates that HDPE sample begins to crystallize at 107°C,[12,22,33–35] which is in agreement with the DSC measurement in Figure 1(b).

The evolution of integrated intensity versus temperature for various bands in the crystallization process is shown in Figure 8. When the temperature is higher than 107°C, the sample of HDPE is in a melting state. Infrared crystalline bands are absent, because there is no existence of crystal lattice. All of the molecular chains are in random coils, and so the absorption of conformational bands with high degree of disorder, like kink (-gtg- or -gtg′-) and double gauche (-gg-), has a strong intensity. With the decrease of temperature, the concentration of -gtg- (or -gtg′-) and -gg- conformers reduces rapidly. At almost the same time, the crystalline bands appear, and the intensity increases quickly. It can be noticed that in the range of 107–101°C, the HDPE sample crystallizes very fast. During the crystallization, some conformational defects, such as kink and double gauche, change into all-trans conformation, which is more stable in the crystalline phase. The enhancing intensity of the crystalline bands means the increasing of all-trans conformation. Note that the intensity change of end-gauche has somewhat difference. Just before the crystallization, the concentration of gauche conformer drops a little, which may be related to the conformational transformation from end-gauche into all-trans, to facilitate the occurrence of crystal nucleation. After the crystallization, more and more nonplanar defects change into the all-trans conformation, and also a small part of non-

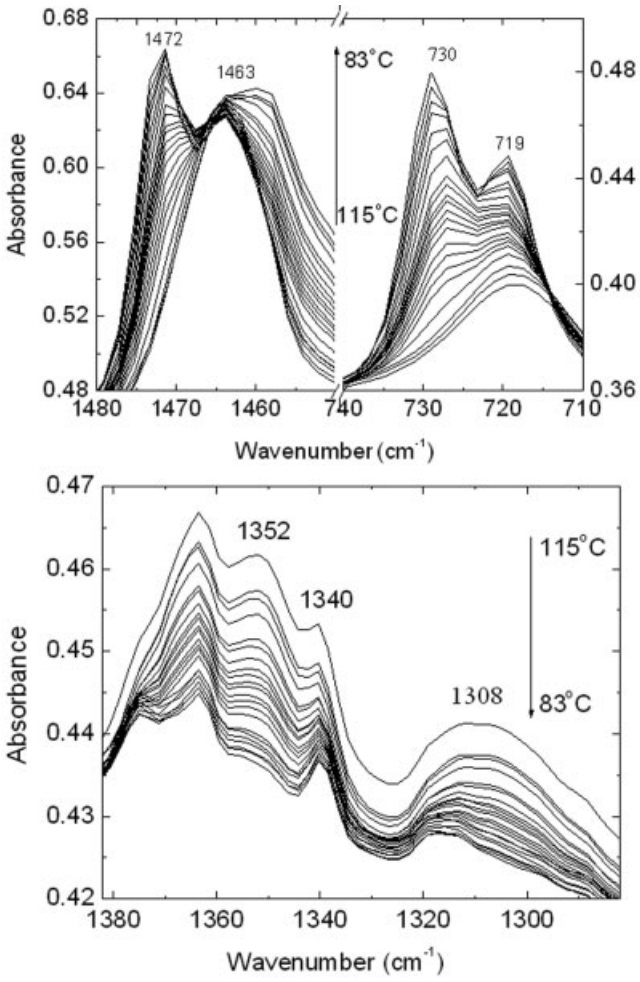

Figure 7 Infrared spectra of HDPE, taken as a function of temperature for the cooling process: (a) two infrared crystalline bands at 1472 and 730 cm^{-1}; (b) three conformational bands at 1340 cm^{-1} (-t_mg), 1308 cm^{-1} (-gtg- and -gtg′-), and 1352 cm^{-1} (-gg-).

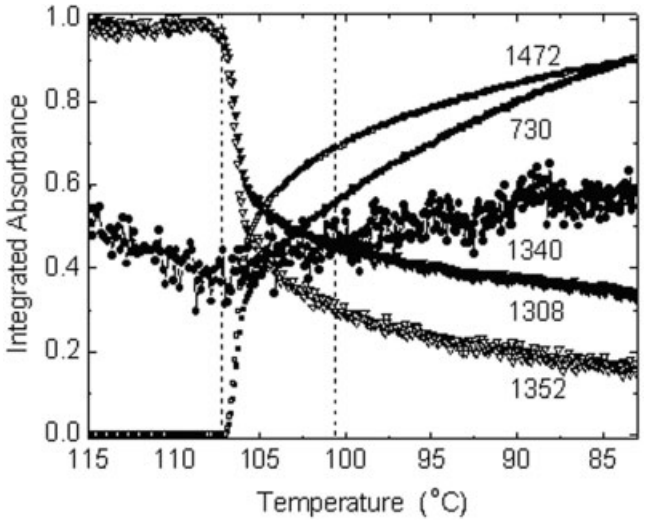

Figure 8 Temperature dependence of integrated absorbance of the bands in the cooling process associated with crystalline phase (■ 730 cm^{-1} and □ 1472 cm^{-1}) and conformational defects [● 1340 cm^{-1}: -t_mg; ▼ 1308 cm^{-1}: -gtg- (kink); and ▽ 1352 cm^{-1}: -gg- (double-gauche)].

planar defects, with high disorder, change into end-gauche, and so the intensity at 1340 cm^{-1} increases. When the temperature is lower than 101°C, the intensity of all bands changes slowly. Furthermore, Figure 9 shows that the ratios of different conformational bands after normalization, such as A_{1340}/A_{1308} and A_{1308}/A_{1352}, increase with the decrease of temperature. It can be inferred that during the crystallization from the melt, -gg- conformation first changes into -gtg- (or -gtg′-), and then into -t_n- and also a small part

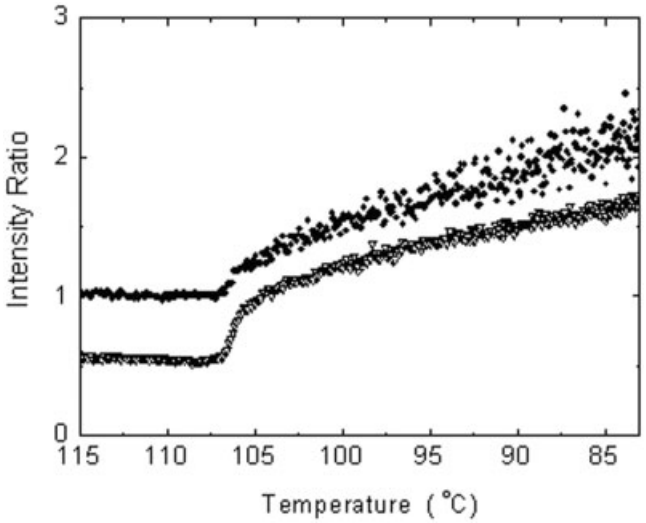

Figure 9 The intensity ratios of different conformational bands versus temperature in the cooling process: ● A_{1340}/A_{1308}: the ratio of end-gauche to kink; ▽ A_{1308}/A_{1352}: the ratio of kink to double gauche.

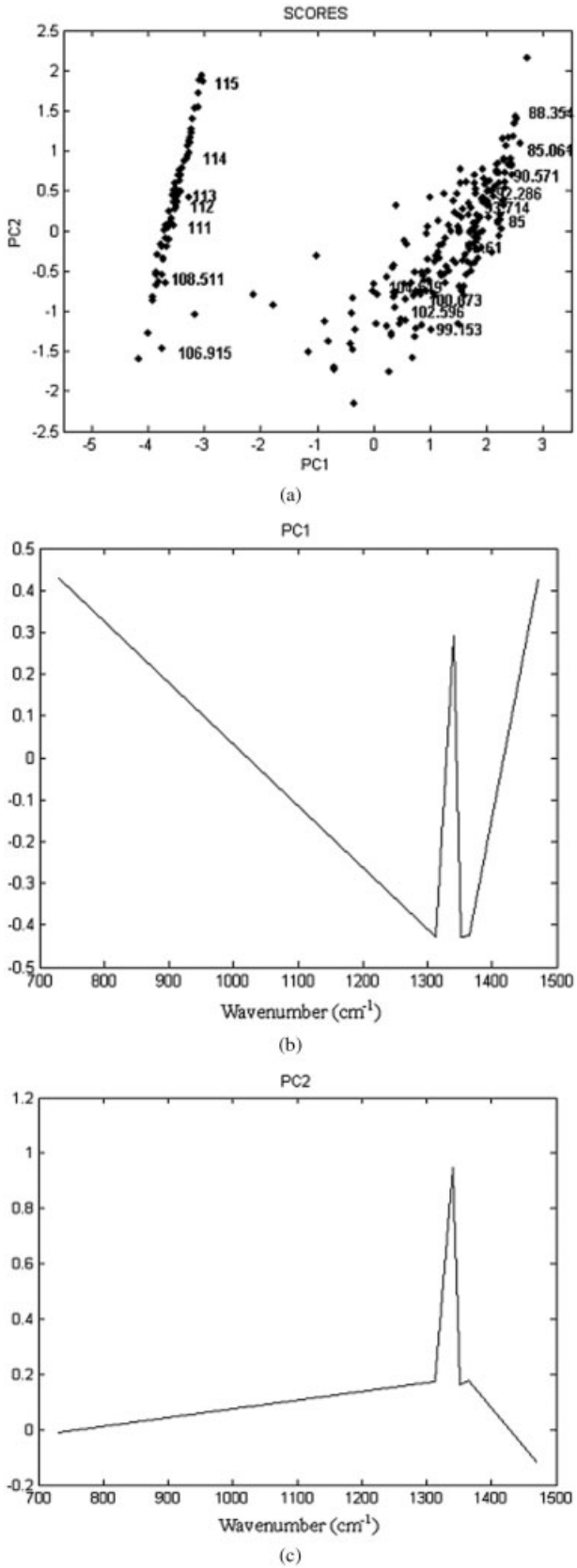

Figure 10 PCA applied to the IR data (a), and plots of PC1 (b), and PC2 (c), during the cooling process.

of -t_mg, which is well in accordance with the degree of the conformational order in HDPE molecular chains.

Figure 10 presents the HDPE cooling scores plot of PC1, which accounts for 89.53% of the variance in the spectral data of the temperature range 115–83°C, against PC2, which accounts for 10.12%. Although the data points below 107°C are a little bit dispersive, it is still very clear that only one major conformational change occurs at the crystallization temperature.

The comparison of conformational changes during the melting and crystallization processes exhibits that, although the polymer crystallization is the reverse process of polymer melting, there still exist some obvious differences in the conformational transformation between them. Restricted by the crystal lattice, the conformational transition of HDPE takes place gradually upon heating, and various conformational transformations can be discerned. However, during the cooling process, HDPE crystallizes very quickly, and only one major conformational transition occurs near the crystallization temperature. To further clarify the conformational change of HDPE crystallization in detail, other online monitoring techniques, such as step-scan time-reserved FTIR and synchrotron radiation, are needed.

CONCLUSIONS

With the aid of time-resolved FTIR spectroscopy, the conformational changes of HDPE during melting and crystallization are studied. Heating the semicrystalline HDPE sample, the various conformational transformations take place gradually. Below 84°C, the major characteristics are the conformational transition from all-trans to end-gauche. When the temperature is higher than 84°C, the mobility of HDPE chains is strengthened greatly. More and more all-trans and end-gauche conformations change into other nonplanar defects with high disorder, such as kink and double-gauche conformers, until the entire melting of the sample.

Above melting point, the sample is in a molten state. The concentration of conformation with high disorder degree, such as kink and double-gauche conformers, is very high, and no crystalline band appears. In the temperature range of 107–101°C, HDPE crystallizes rapidly. All the absorption of the conformational defects drops quickly, except for the end-gauche conformation, which increases slightly after crystallization. At the same time, the intensity of the crystalline bands, representing the concentration of all-trans conformation, increases rapidly. Finally, as the temperature is lower than 101°C, the macromolecular chains become much more in order with decreasing the temperature, and the all-trans conformation is dominant in low temperature.

References

1. Keller, A. Philos Mag 1957, 2, 1171.
2. Till, P. H. J Polym Sci 1957, 24, 30.
3. Fisher, E. W. Kolloidn Zh 1958, 159, 108.
4. Hoffman, J. D.; Miller, R. L. Polymer 1997, 38, 3151.
5. Wunderlich, B.; Metha, A. J Phys Chem B 1974, 12, 255.
6. Sadler, D. M. Nature 1987, 326, 174.
7. Imai, M.; Kaji, K.; Kanaya, T. Macromolecules 1994, 27, 7103.
8. Strobl, G. Eur Phys J E 2000, 3, 165.
9. Stein, R. S.; Norris, F. H. J Polym Sci 1956, 21, 381.
10. Stroble, G.; Ewen, B.; Fischer, E. W.; Piesczck, W. J Chem Phys 1974, 61, 5257.
11. Liang, C. Y.; Krimm, S.; Sutherland, G. B. B. M. J Chem Phys 1956, 25, 543.
12. Tashiro, K.; Sasaki, S. Prog Polym Sci 2003, 28, 451.
13. Okada, T.; Mandelkern, L. J Polym Sci 1967, 5, 239.
14. Snyder, R. G. J Chem Phys 1967, 47, 1316.
15. Schultz, J. M. J Polym Sci Polym Phys Ed 1976, 14, 2291.
16. Strobl, G.; Schneider, M. Macromolecules 1980, 18, 1343.
17. Hikosaka, M.; Rastogi, S.; Keller, A.; Kawabata, H. J Macromol Sci Phys 1992, 31, 87.
18. Snyder, R. G.; Maroncelli, M.; Qi, S. P.; Strauss, H. L. Science 1981, 214, 188.
19. Maroncelli, M.; Qi, S. P.; Strauss, H. L.; Snyder, R. G. J Am Chem Soc 1982, 104, 6237.
20. Hagemann, H.; Strauss, H. L.; Snyder, R. G. Macromolecules 1987, 20, 2810.
21. Koenig, J. L. Probing Polymer Structures; American Chemical Society: Washington, DC, 1979; p 104.
22. Tashiro, K.; Sasaki, S.; Gose, N.; Kobayashi, M. Polym J 1998, 30, 485.
23. Tashiro, K.; Stein, R. S.; Hsu, S. L. Macromolecules 1992, 25, 1801.
24. Zhu, X. Y.; Yan, D. Y.; Yao, H. X.; Zhu, P. F. Macromol Rapid Commun 2000, 21, 354.
25. Zhu, X. Y.; Yan, D. Y.; Fang, Y. P. J Phys Chem B 2001, 105, 12461.
26. Zhu, X. Y.; Yan, D. Y.; Fang, Y. P.; Chen, L. Appl Spectrosc 2003, 57, 104.
27. Zhu, X. Y.; Fang, Y. P.; Yan, D. Y. Polymer 2001, 42, 8595.
28. Zhu, X. Y.; Li, Y. J.; Yan, D. Y.; Lu, Q. H.; Zhu, P. F. Colloid Polym Sci 2001, 279, 292.
29. Zhu, X. Y.; Fang, Y. P.; Li, Y. J.; Yan, D. Y.; Zhu, P. F.; Lu, Q. H. Chem J Chin Univ 2001, 22, 1425.
30. Kobayashi, M.; Akita, K.; Tadokoro, H. Makromol Chem 1968, 118, 324.
31. Zerbi, G.; Ciampelli, F.; Zamboni, V. J Polym Sci Part C: Polym Symp 1964, 7, 141.
32. Xiao, Y.; Zhu, X. Y.; Chen, L.; He, P.; Yan, D. Y.; Wang, X. A. J Polym Sci Part B: Polym Phys 2004, 42, 60.
33. Hagemann, H.; Snyder, R. G.; Peacock, A. J.; Mandeldern, L. Macromolecules 1989, 22, 3600.
34. Painter, P. C.; Havens, J.; Hart, W. W.; Koenig, J. L. J Polym Sci Polym Phys Ed 1977, 15, 1237.
35. Androsch, R.; Kolesov, I.; Radusch, H.-J. J Therm Anal Cal 2003, 73, 59.
36. Ozzetti, R. A.; Pedro de Oliveira Filho, A.; Schuchardt, U.; Mandelli, D. J Appl Polym Sci 2002, 85, 734.
37. Martens, H.; Naes, T. Multivariate Calibration; Wiley: Chichester, UK, 1998.
38. Hamerton, I.; Hay, J. N.; Herman, H.; Howlin, B. J.; Jepson, P.; Gillies, D. G. J Appl Polym Sci 2002, 84, 2411.
39. He, P.; Xiao, Y.; Zhang, P. M.; Zhu, N.; Zhu, X. Y.; Yan, D. Y. Appl Spectrosc 2005, 59, 33.
40. He, P.; Xiao, Y.; Zhang, P. M.; Xing, C. H.; Zhu, N.; Zhu, X. Y.; Yan, D. Y. Polym Degrad Stab 2005, 88, 473.
41. Zhu, X. Y.; Yan, D. Y. Macromol Chem Phys 2001, 202, 1109.
42. Zhang, F.; Qiu, W.; Yang, L.; Endo, T.; Hirotsu, T. J Appl Polym Sci 2003, 89, 3292.
43. Huang, Z.; Marand, H.; Cheung, W. Y.; Guest, M. Macromolecules 2004, 37, 9922.
44. Tashiro, K.; Gose, N. Polymer 2001, 42, 8987.